

Biological and Chemical Response of the Equatorial Pacific Ocean to the 1997–98 El Niño

F. P. Chavez,^{1*} P. G. Strutton,¹ G. E. Friederich,¹ R. A. Feely,²
G. C. Feldman,³ D. G. Foley,⁴ M. J. McPhaden²

During the 1997–98 El Niño, the equatorial Pacific Ocean retained 0.7×10^{15} grams of carbon that normally would have been lost to the atmosphere as carbon dioxide. The surface ocean became impoverished in plant nutrients, and chlorophyll concentrations were the lowest on record. A dramatic recovery occurred in mid-1998, the system became highly productive, analogous to coastal environments, and carbon dioxide flux out of the ocean was again high. The spatial extent of the phytoplankton bloom that followed recovery from El Niño was the largest ever observed for the equatorial Pacific. These chemical and ecological perturbations were linked to changes in the upwelling of nutrient-enriched waters. The description and explanation of these dynamic changes would not have been possible without an observing system that combines biological, chemical, and physical sensors on moorings with remote sensing of chlorophyll.

Upwelling of waters enriched in nutrients and carbon dioxide (CO_2) occurs in the equatorial Pacific Ocean from the coast of South America to beyond the international date line. The vast area involved makes this region the largest natural oceanic source of atmospheric CO_2 . Physical processes and biological consumption determine the strength of this source, which varies considerably from year to year (1). The primary source of interannual variability is El Niño. In 1997, bio-optical and chemical sensors were added to moorings of the Tropical Atmosphere Ocean (TAO) array (2), and the Sea-viewing Wide Field-of-view Sensor (SeaWiFS), a satellite-based ocean color sensor (3), was launched. Serendipitously, a very strong El Niño developed during 1997 and matured late in the year (4). A dramatic recovery that led to a cold La Niña condition began in mid-1998. Here we combine the biological and chemical information from the moorings and SeaWiFS with the physical data from the TAO array and data collected from ships that service the array to describe the bio-

logical-physical coupling in the equatorial Pacific. These observations allowed us to quantify the effects of zonal wind anomalies, Kelvin waves, thermocline anomalies, advection of oligotrophic waters, tropical instability waves (TIWs), and variations in the strength and depth of the equatorial undercurrent (EUC) on primary production (PP) and air-sea CO_2 flux.

The Physical Environment

Normally, trade wind-driven upwelling creates a tongue of cold surface water along the equator, from the coast of South America to the international date line (Fig. 1C). The source of this upwelled water is the EUC, which flows eastward across the basin at a depth of 20 to 200 m (5). Every 3 to 7 years, the central and eastern equatorial Pacific warms dramatically as El Niño develops (Fig. 1). The 1997–98 El Niño was, by some measures, the strongest of the 20th century (4, 6). A weakening and reversal of the trade winds in the western and central equatorial Pacific preceded the rapid development of unusually warm sea surface temperatures (SST) east of the international date line in early 1997 (Fig. 2). These wind anomalies, which appeared as a series of westerly events of either increasing intensity or fetch, or both, along the equator (Fig. 2A), were the manifestation of the Madden and Julian Oscillation (MJO), a 30- to 60-day wave in the atmosphere originating over the Indian Ocean (7–9). The westerly wind events excited equatorial Kelvin waves that propagated eastward

across the basin in 1 to 2 months, ultimately depressing the thermocline in the eastern Pacific by over 90 m in late 1997 (Fig. 2B). A depressed thermocline favors development of warm surface temperatures because the cold water reservoir that feeds upwelling in the equatorial cold tongue deepens (10, 11).

Conversely, in the western Pacific, the thermocline anomalously shoaled by 20 to 40 m in 1997 as Rossby waves, generated by the relaxation of the trade winds, propagated westward toward Indonesia and New Guinea. Western Pacific SSTs decreased, probably in part because of unusually high evaporative heat loss across the air-sea interface and greater oceanic mixing of cold subsurface waters caused by MJO-generated ocean turbulence (12–15). The net result of these processes on ocean thermal structure was to flatten the thermocline along the equator and eliminate the normal east-west SST gradient (Table 1). The western Pacific warm pool [surface waters greater than about 28°C (16)] migrated eastward with the collapse of the trade winds, and the equatorial cold tongue (the strip of cold water indicative of equatorial upwelling) failed to develop in boreal summer and fall (Figs. 1 and 2). At the height of the event, in December 1997, 28° to 29°C water covered the equatorial basin, and SST anomalies exceeded 5°C at some locations in the region normally occupied by the cold tongue. Low-level westerly winds associated with the MJO drive warm water eastward near the equator (16–18) and generate local downwelling instead of the normal upwelling. The strongest westerly surface winds in our observations were apparent over waters above $\sim 29^\circ\text{C}$ (Fig. 2):

In early 1998, westerly wind anomalies along the equator weakened and migrated eastward with the pool of 29°C water, and easterly wind anomalies appeared in the far western Pacific. Thermocline shoaling progressed slowly into the central and eastern Pacific, although SSTs remained unusually high where the trade winds were weak (Fig. 2). It was not until the trade winds abruptly returned to near normal strength in the eastern Pacific in mid-May 1998 that the cold subsurface waters could be upwelled efficiently into the surface layer. Subsequently, SSTs in some areas of the equatorial cold tongue plummeted 8°C during May and June and the El Niño was brought to an abrupt end (4). Cold conditions continued through the remainder of the year, expanding both east and west along the equator.

Air-Sea Flux of CO_2

The surface waters of the central and eastern equatorial Pacific are characterized by high partial pressure of carbon dioxide ($p\text{CO}_2$) and

¹Monterey Bay Aquarium Research Institute, 7700 Sandholdt Road, Moss Landing, CA 95039, USA. E-mail: chfr@mbari.org. ²National Oceanic and Atmospheric Administration Pacific Marine Environmental Laboratory, 7600 Sand Point Way NE, Seattle, WA 98115, USA. ³NASA/Goddard Space Flight Center, Code 970.2, Greenbelt, MD 20771, USA. ⁴National Marine Fisheries Service Honolulu Laboratory, 2570 Dole Street, Honolulu, HI 96822–2396, USA.

*To whom correspondence should be addressed: E-mail: chfr@mbari.org

Fig. 1. Advanced Very High Resolution Radiometer (AVHRR) SST and SeaWiFS chlorophyll comparisons for January and July 1998. SST anomalies in January 1998 were close to the highest observed during the El Niño. There is little or no evidence of the equatorial cold tongue (A) or of enhanced chlorophyll along the equator (B). In sharp contrast, by July 1998, a dramatic recovery had taken place. There is a well-developed cold tongue (C) and a dramatic bloom of phytoplankton (D) along the equator. High chlorophyll concentrations ($>1 \mu\text{g liter}^{-1}$) had not previously been observed over such a large area. The filled circles at 0° , 155°W ; 2°S , 170°W ; and 2°N , 110°W mark the locations of TAO moorings instrumented with biochemical sensors. The white lines represent the sections occupied by ships that service the TAO array, from which data are presented in this paper.

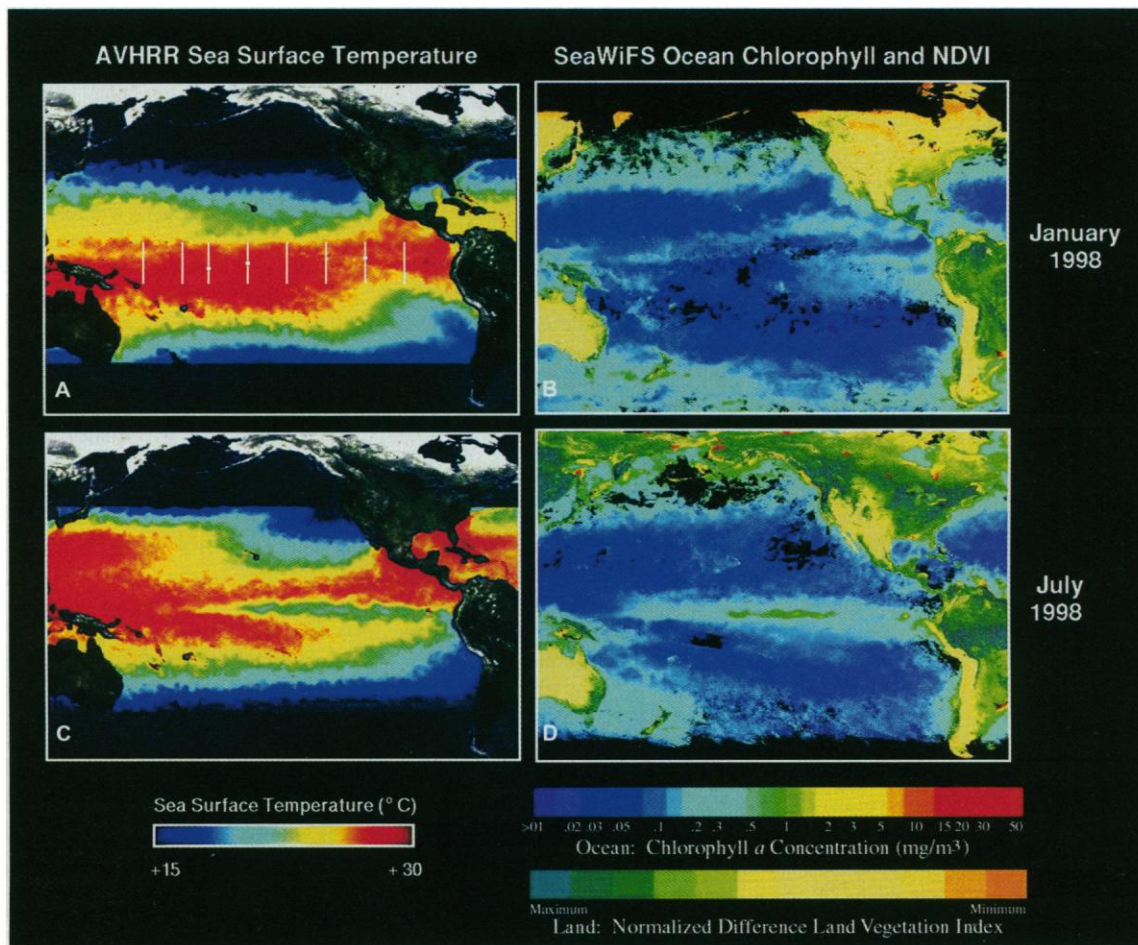
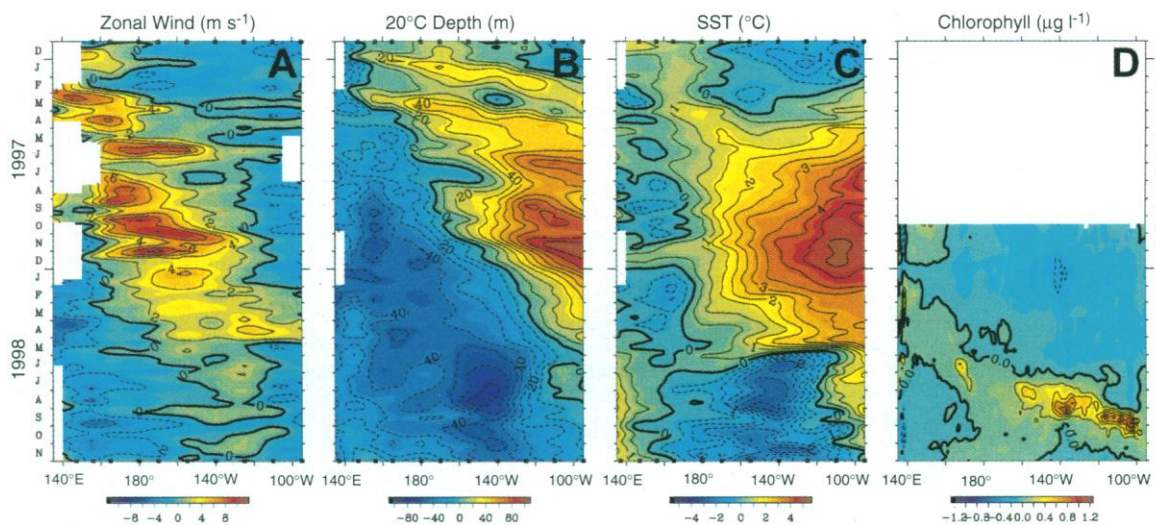


Fig. 2. Time-longitude sections of anomalies in (A) surface zonal winds (in meters per second), (B) 20°C isotherm depth (in meters), (C) SST (in degrees Celsius), and (D) SeaWiFS chlorophyll (in micrograms per liter) for 24 months ending in November 1998. Analysis is based on 5-day averages between 2°N and 2°S of moored time series data from the TAO array and on 8-day SeaWiFS composites. Anomalies are relative to monthly climatologies fitted with a cubic spline to 5-day intervals for TAO array data and relative to the full record for SeaWiFS. Squares on the abscissas indicate longitudes where TAO data were available. Major anomalies in the western Pacific wind field occurred on a 30- to 60-day cycle (7) beginning in December 1996. Bursts of westerlies generated Kelvin waves that propagated across the Pacific at over 200 km day^{-1} , as evident in the depth of the 20°C isotherm. The zonal wind anomalies migrated across the Pacific and reached the eastern Pacific early in 1998. The 20°C anomalies reached their peak in the eastern Pacific in late 1997 and



began recovery in the central Pacific early in 1998, well before the SST. The SST anomalies lagged the subsurface perturbations early in the event, became notable after April 1997, reached their peak in late 1997 and early 1998, and recovered dramatically in late May 1998 when the trade winds resumed. Chlorophyll was low in the central and eastern Pacific and high in the western Pacific in late 1997 and early 1998. High chlorophyll ($\sim 1 \mu\text{g liter}^{-1}$) appeared in the central Pacific in July and August 1998 and propagated eastward at 1.2 m s^{-1} .

nutrient (nitrate, phosphate, and silicate) concentrations resulting from shallow equatorial upwelling. Equatorial upwelling annually supplies about 0.7 to 1.5 Pg (10^{15} g) of carbon as CO_2 to the atmosphere and is the atmosphere's largest oceanic source (19–21). The equatorial Pacific contributes about four times as much CO_2 to the atmosphere as the combined fluxes of the rest of the oceanic equatorial regions (21). A comprehensive set of atmospheric and surface ocean pCO_2 (1); nitrate, chlorophyll, and PP (22); and supporting hydrographic data were obtained during the mature phase of the 1997–98 El Niño (November 1997 to May 1998) and compared with data collected during non-El Niño conditions (Fig. 3).

Previous modeling and field studies of seawater pCO_2 in this region have emphasized interannual variability (1, 23–31). The non-El Niño data indicate much higher ΔpCO_2 (ocean minus atmosphere) values than the corresponding values for the mature phase of the 1997–98 El Niño (Fig. 3 and Table 1). The variability in ΔpCO_2 was driven entirely by variations in seawater

pCO_2 . Although values close to equilibrium were observed north and south of the equator in the western part of the study region, the region between 6°N and 8°S had a large positive ΔpCO_2 centered on the equator across the entire basin during 1995–96 (Fig. 3). The bulk of equatorial upwelling takes place in a box 5°N to 5°S and 90°W to 180° (32). The high ΔpCO_2 found north, south, and west of this box reflects advection of waters high in pCO_2 out of this region. In contrast, the 1997–98 data indicate near-equilibrium ΔpCO_2 values for the same region. These distributions of ΔpCO_2 in the eastern Pacific show the largest interannual variability (100 to 120 μatm) since the 1982–83 El Niño (1).

The properties of the water column in the eastern equatorial Pacific during and after the 1997–98 El Niño–Southern Oscillation event explain the variability of ΔpCO_2 . Mooring time series of ΔpCO_2 (Fig. 4) show that during the mature phase of El Niño, in late 1997 and early 1998, the surface water pCO_2 was on average below atmospheric levels and the equatorial Pacific at 0°, 155°W was a sink for atmospheric

CO_2 . Strong eastward currents associated with the migration of the warm pool caused the 0°, 155°W mooring to be pulled underwater in March 1998, leading to instrument failure. The mooring was redeployed in June 1998. By this time, recovery from El Niño had begun, and high surface water pCO_2 was measured at 0°, 155°W. The recovery at 2°S, 170°W occurred later, and, during June 1998, waters low in pCO_2 were found at this site. These values increased rapidly in July, followed by large excursions associated with the passage of TIWs (Figs. 4 and 5).

El Niño produces large interannual effects on ocean-atmosphere CO_2 exchange in the equatorial Pacific (Fig. 3, C and D). Between the non-El Niño conditions of 1995–96 and the mature El Niño period during 1997–98, the average CO_2 flux from 10°S to 10°N and 80°W to 135°E decreased from about 2.0 to 0.3 mol C m^{-2} year $^{-1}$. The high CO_2 fluxes in 1995–96 were due to increased surface water pCO_2 and higher winds (Table 1). The EUC was much closer to the surface in 1995–96, and upwelling supplied the higher pCO_2 found in surface waters. We calculate that for the 1-year period of 1995–96, about 0.9 (± 0.6) Pg of C as CO_2 was released to the atmosphere over the 10°S to 10°N and 80°W to 135°E area. In sharp contrast, for the 1-year period between the spring of 1997 and the spring of 1998, the CO_2 flux to the atmosphere was about 0.2 (± 0.14) Pg of C over the same region. Thus, the amount of CO_2 retained in the equatorial oceans during the 1997–98 El Niño period (that is, 0.7 Pg of C year $^{-1}$) was similar to that of the strong El Niño of 1982–83 (1).

We also calculated CO_2 fluxes from the buoy-measured ΔpCO_2 and winds (Fig. 4C). The fluxes during the mature El Niño phase averaged 0.20 (± 0.15) mol of C m^{-2} year $^{-1}$ into the ocean. After recovery from El Niño, these values ranged from 2 to 6 mol of C m^{-2} year $^{-1}$ out of the ocean, including large weekly variations in flux, driven by changes in wind speed, that are not in the ship survey calculations (Fig. 4). From the mooring data, we calculate an average flux of 3.5 (± 1.86) mol of C m^{-2} year $^{-1}$ out of the ocean for the cold period after recovery from El Niño. If this is the average flux in the 5°N to 5°S and 90°W to 180° region of active upwelling, then 0.47 Pg of C year $^{-1}$ is released into the atmosphere during non-El Niño conditions. This value compares well with the shipboard estimate of 0.38 Pg of C year $^{-1}$ for the same area. This calculation suggests that during non-El Niño conditions, on the order of 50% of the nutrients and CO_2 upwelled in the equatorial Pacific are advected out of the region of active upwelling before being consumed by biological processes or lost to the atmosphere.

Table 1. Comparison of physical, chemical, and biological conditions in the central equatorial Pacific for mean, El Niño onset, El Niño mature, and La Niña.

Condition	Physics	Chemistry	Biology
Mean	Upwelling-favorable trade winds; deep thermocline in west, shallow in east; cold tongue; strong undercurrent	Elevated macronutrients (NO_3 , PO_4 , SiO_4 , and CO_2); flux of CO_2 out of ocean; iron limitation	Chlorophyll ~ 0.2 to 0.3 μg per liter $^{-1}$; picoplankton dominated; primary production (PP) ~ 75 mmol C m^{-2} day $^{-1}$; new production (NP) $\sim 15\%$ of PP
El Niño onset	Upwelling-favorable trade winds; strong Kelvin waves; thermocline deepens in central and eastern Pacific; reduced cold tongue; variable undercurrent	Elevated (but lower than mean) macronutrients; flux of CO_2 out of ocean; stronger iron limitation	Chlorophyll < 0.2 μg liter $^{-1}$; picoplankton dominated; PP ~ 50 mmol C m^{-2} day $^{-1}$; NP $\sim 10\%$ of PP
El Niño mature	Weak trade winds, reduced upwelling; enhanced rainfall; flat thermocline across basin, recovering in central and eastern Pacific before SST; no cold tongue; weak undercurrent	No enhancement of macronutrients; oligotrophic conditions; flux of CO_2 close to zero	Chlorophyll ~ 0.05 μg liter $^{-1}$; picoplankton dominated; PP ~ 35 mmol C m^{-2} day $^{-1}$; NP $\sim 10\%$ of PP
La Niña	Upwelling-favorable trade winds; shallow thermocline in central Pacific; enhanced cold tongue; strong undercurrent	Elevated (higher than mean) macronutrients; flux of CO_2 out of ocean (stronger than mean); enhanced supply of iron	Chlorophyll < 1 μg liter $^{-1}$, higher in blooms; diatoms important; PP ~ 80 reaching 160 mmol C m^{-2} day $^{-1}$ in blooms; NP $\sim 15\%$ of PP, up to 50% in blooms

Nitrate and Chlorophyll Fluctuations

High concentrations of nitrate, phosphate, and silicate in the equatorial Pacific lead to unexpectedly small increases in chlorophyll (33). This low productivity contributes directly to the loss of upwelled CO₂ to the atmosphere. Small-scale iron fertilization experiments have shown that the low productivity can result from iron limitation (34, 35). In January 1997, nitrate and chlorophyll concentrations at 0°, 155°W were 5 μM and 0.2 μg liter⁻¹, respectively—typical for the equatorial Pacific (22) (Figs. 3 and 4 and Table 1). The passage of downwelling Kelvin waves in January, March, and April 1997 resulted in chlorophyll fluctuations, even though substantive amounts

of nitrate were measured at the surface (2). Intraseasonal Kelvin waves, which altered the depth of the EUC, the thermocline, and therefore the concentration of iron in upwelled water, were the primary agents affecting PP during onset of this El Niño (2).

In early May 1997, the 28°C SST isotherm passed the mooring site at 0°, 155°W, and at this time, nitrate and chlorophyll concentrations reached 3 μM and 0.1 μg liter⁻¹, respectively. Conceptual models developed from observations in the eastern tropical Pacific (36, 37) have suggested that Kelvin waves are the primary agents affecting biological productivity, because upwelling-favorable winds are maintained in this region. The upwelled

waters are low in nutrients, and productivity is hence reduced. Indeed, during weak to moderate events, zonal wind anomalies are restricted to the western Pacific, and hence Kelvin waves are the dominant source of the biogeochemical perturbations in the central Pacific (38). However, during the strong 1997–98 event, eastward migration of the zonal wind anomalies extended into the eastern equatorial Pacific (Figs. 2 and 4), shutting down local upwelling in the central equatorial Pacific for several months.

In the absence of upwelling, nutrient concentrations declined, and in November 1997, close to the peak of the event, nitrate and chlorophyll at 0°, 155°W were less

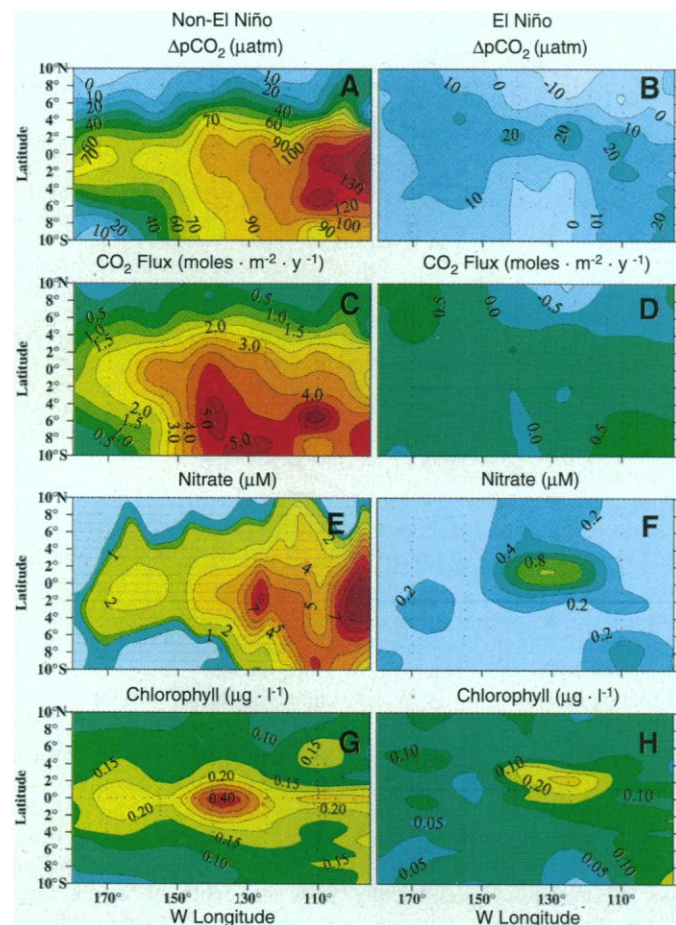
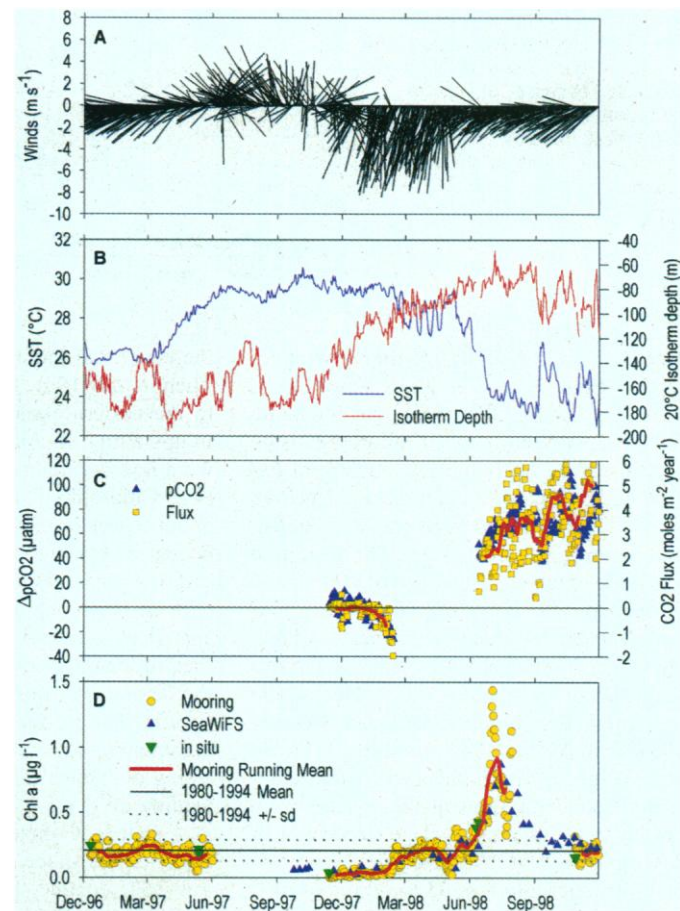
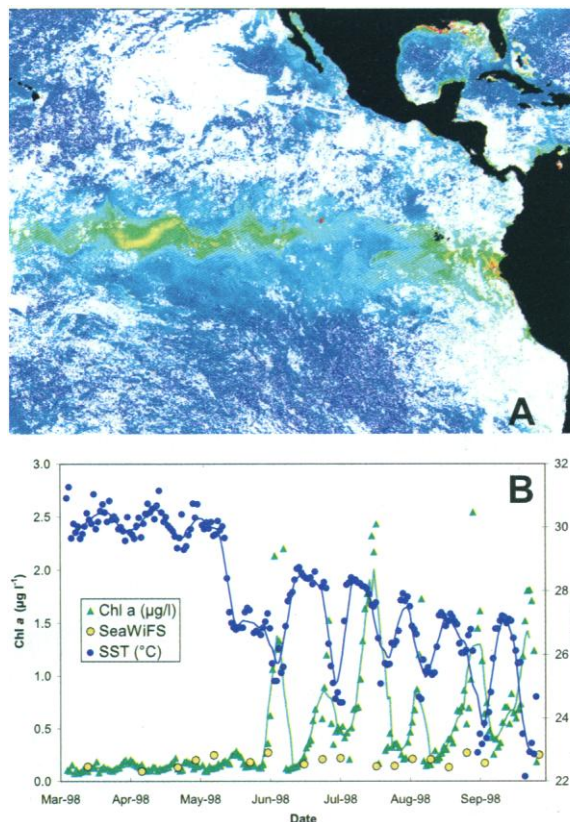


Fig. 3 (left). Maps of the distribution of $\Delta p\text{CO}_2$ (in microatmospheres) and CO₂ flux (in moles per square meter per year) in the central and eastern equatorial Pacific during the 1995–96 non-El Niño (A and C) and the 1997–98 El Niño event (B and D). Maps of nitrate (in micromolar) from Levitus climatology (E) and during the 1997–98 event (F). Maps of surface chlorophyll (in micrograms per liter) from climatology (22) (G) and the 1997–98 El Niño event (H). Underway atmospheric and surface ocean pCO₂ measurements, nitrate, chlorophyll, and supporting hydrographic data were obtained during cruises on the NOAA Ship *Ka'imimoana*, which services the TAO array (Fig. 1A). **Fig. 4 (right).** Time series of winds (A), SST and 20°C isotherm depth (B), $\Delta p\text{CO}_2$ and CO₂ flux (red line is 21-day running mean) (C), and chlorophyll (Chl) (D) measured on a mooring at 0°, 155°W. SeaWiFS chlorophyll, ship chlorophyll from the same location, and the long-term mean equatorial Pacific ship chlorophyll are also plotted in (D). Winds remained favorable for



upwelling until early 1997, became southerly and variable through late in the year, and then turned northerly until May 1998 when the northeast trade winds resumed. SST remained at mean levels until April 1997, when it rose to ~30°C by June 1997, where it remained, with wave-like excursions in early 1998, until May 1998, when it dropped precipitously. Positive $\Delta p\text{CO}_2$ and CO₂ flux indicate that ocean is higher than atmosphere and flux is out of the ocean, respectively. During the height of the event, $\Delta p\text{CO}_2$ and CO₂ flux were close to zero, and the average flux was into the ocean. After recovery, $\Delta p\text{CO}_2$ was close to 80 μatm and flux was out of the ocean. Chlorophyll fluctuations (driven by Kelvin waves) were observed in early 1997. By late 1997 and early 1998, chlorophyll had decreased to around 0.05 μg liter⁻¹, where it remained until April 1998 when it returned to mean values. A bloom was observed in July 1998. Long-term mean levels were observed after the bloom. Note the correspondence between ship, mooring, and SeaWiFS chlorophyll data.

Fig. 5. SeaWiFS composite of chlorophyll for the week of 12 to 19 July 1998 (A) and time series of mooring-derived chlorophyll and SST and 8-day, 9-km SeaWiFS chlorophyll from 2°N, 110°W (B). A wavelength of 1000 km was estimated from the cusps in the distorted high chlorophyll of the SeaWiFS image associated with TIWs. A period of about 21 days was estimated from the SST and chlorophyll time series, resulting in a propagation speed of 50 km day⁻¹, characteristic of TIWs. The rapid fluctuations in mooring-derived chlorophyll at 2°N, 110°W were associated with the rapid temperature gradient (rather than the coldest waters) at the leading edge of the TIWs. The blooms were not evident in the SeaWiFS data probably because of spatio-temporal averaging, suggesting that these blooms might be the narrow "lines in the sea" reported by Yoder *et al.* (51).



than 0.05 µM and 0.05 µg liter⁻¹, respectively (Figs. 3 and 4 and Table 1). In contrast, during the weak to moderate 1991–92 El Niño, unused nitrate persisted at the surface in the central equatorial Pacific (22). The conditions during 1997–98 resembled those observed in the oligotrophic subtropical gyres (39). The depletion of nitrate extended to a depth of 100 m, and primary productivity was now nitrate limited. The lateral extent of nitrate depletion is evident from a comparison of the Levitus climatological nitrate field with in situ measurements obtained between October 1997 and April 1998, spanning 95°W to 180° (Fig. 3). The typically elevated chlorophyll concentrations at the equator were present only as a subsurface maximum of 0.2 µg liter⁻¹ at 100-m depth. Mean primary productivity was 35 to 40 mmol of C m⁻² day⁻¹—about half the climatological mean (22) (Table 1). The decrease in primary production from the normal 3.65 Pg of C year⁻¹ (22) in the 5°N to 5°S, 90°W to 180° region of active upwelling was 1.8 Pg of C year⁻¹, or 4 to 5% of global ocean primary production (40). On the basis of the reduction in upwelling, we estimate the decrease in potential new production to be about 0.8 Pg of C year⁻¹, or 10% of global new production (41).

The phytoplankton community began to recover in April 1998, and chlorophyll returned to concentrations that are typical for

the equatorial Pacific cold tongue (Fig. 4). Then in May 1998, the trade winds resumed in the eastern equatorial Pacific, resulting in upwelling of cold subsurface waters that were now anomalously close to the surface (4). Chlorophyll increased dramatically, about 3 weeks after the rapid temperature decrease. At some locations along the equator, the eventual increase in chlorophyll was on the order of 40-fold (Fig. 4). The spatial extent of the phytoplankton bloom that followed recovery from El Niño was the largest ever observed for the equatorial Pacific. The recovery of the phytoplankton community was accompanied by two interesting dynamical phenomena: (i) the propagation of TIWs (38, 42) from east to west at a speed of about 50 km day⁻¹, which distorted the shape of the high-chlorophyll/low-SST tongue because of meridional transport associated with the wave propagation (Fig. 5), and (ii) the migration of a patch of high chlorophyll concentration (up to ~2 µg liter⁻¹ as calculated by the SeaWiFS OC2V2 algorithm) from west to east (Fig. 2) at a velocity of 105 (±5) km day⁻¹ (~1.2 m s⁻¹). This patch was constrained within the central region of the propagating TIWs, and its eastward movement did not appear to be a direct result of fluctuations in zonal winds, SST, or thermocline depth (as determined by the depth of the 20°C isotherm). Acoustic Doppler current profiler data from 0°, 140°W and 0°, 170°W

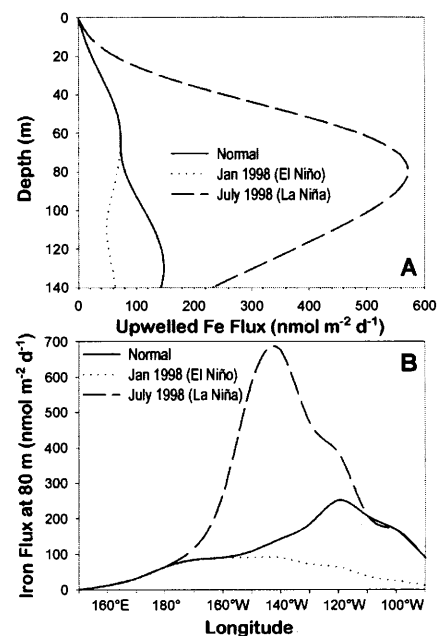
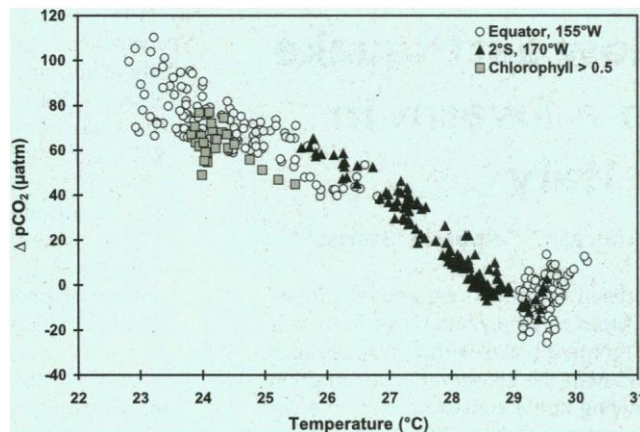


Fig. 6. Flux of iron during normal, El Niño, and La Niña conditions. The upwelling rate reported by Gordon *et al.* (43) was used for all of the 140°W simulations (A). For the longitudinal simulations, the upwelling rates reported by Chai *et al.* (49) were used (B). Upwelling during the mature phase of the 1997–98 El Niño was substantially reduced so flux of iron was close to zero and is not reflected in the graphs. The iron vertical profile of Gordon *et al.* (43) for 0°, 140°W was moved vertically depending on depth of the 20°C isotherm (Fig. 2B). A strong enhancement of iron flux in the central Pacific during La Niña is predicted.

show that the EUC was essentially absent during the height of the El Niño event but resumed, strengthened, and shoaled beginning in January 1998, reaching a west to east speed of ~1.4 m s⁻¹ and a depth of 50 to 75 m by June 1998.

We calculated the flux of iron for normal, El Niño, and La Niña conditions (Fig. 6). Inputs for the calculation were the vertical iron distribution reported by Gordon *et al.* (43), the depth of the thermocline (Fig. 2), and the average vertical upwelling profile. We assumed that the iron profile moved vertically with the depth of the thermocline. On the basis of an Fe:C of 1:200,000 (44, 45), we estimate that 13 mmol of C m⁻² day⁻¹ of new production could be supported during normal conditions from the 80-m iron flux. This value agrees well with values measured for the equatorial Pacific (46). In August 1998, when the thermocline was 80 m shallower than normal (Fig. 2), the flux of iron at 80 m increased by an order of magnitude relative to mean conditions (Fig. 6). The modeled iron flux would then support 97 mmol of C m⁻² day⁻¹ of new production, very similar to values measured during a bloom induced

Fig. 7. Scatter diagram of SST and $\Delta p\text{CO}_2$ for the mooring records at 0° , 155°W (open circles) and 2°S , 170°W (filled triangles). The filled squares represent the 0° , 155°W bloom period when lower $\Delta p\text{CO}_2$ was observed, presumably because of increased biological uptake. The statistics of the SST, $\Delta p\text{CO}_2$ relation suggest that $\Delta p\text{CO}_2$ ($r^2 = 0.92$) can be estimated from SST with a standard error of ~ 10 ppm in the region of active upwelling.



by iron fertilization (47). If the new production were converted to phytoplankton biomass at $1 \mu\text{g}$ of chlorophyll per liter per $1 \mu\text{M}$ of N (48), then during normal conditions $0.03 \mu\text{g}$ of chlorophyll per liter would accumulate daily compared with $0.20 \mu\text{g}$ of chlorophyll per liter during the strongest La Niña conditions. If the uptake and biomass accumulation were restricted to the upper 20 m, as is typically seen under bloom conditions, then $0.80 \mu\text{g}$ of chlorophyll per liter could accumulate daily during La Niña. To reach $1.0 \mu\text{g}$ of chlorophyll per liter at the surface from the average of $0.2 \mu\text{g}$ of chlorophyll per liter would take more than 26 days during normal conditions. During La Niña, this concentration could be reached in 1 to 4 days, again similar to what was observed during iron fertilization (35). In support of rapid bloom formation, the drawdown of CO_2 during the 0° , 155°W bloom ($20 \mu\text{atm}$; Fig. 7) is equivalent to an uptake of $\sim 1.5 \mu\text{M}$ of nitrate and generation of $1.5 \mu\text{g}$ of chlorophyll per liter. Observations in early July 1998 (Fig. 7) show that short-term biological effects on $p\text{CO}_2$ cannot be neglected in the equatorial Pacific.

During normal conditions, the thermocline (and nutricline) exhibits a steady gradient from about 200 m in the western Pacific to 50 m or less in the eastern Pacific (Table 1). Zonal winds and upwelling are stronger in the central Pacific (49), counteracting the shallower nutricline depth in the eastern Pacific and producing a relatively even distribution of iron (and macro-nutrient) flux from 90° to 170°W , with a slight enhancement at 120°W (Fig. 6B). During La Niña, when the thermocline in the central equatorial Pacific was abnormally shallow (Fig. 2), iron flux was enhanced dramatically in this region relative to normal conditions (Fig. 6B). The propagation speed of the high chlorophyll patch eastward is similar to the speed of the EUC, suggesting that the iron that first stimulated

productivity in the central Pacific and the resulting bloom may have been advected eastward by a near-surface EUC.

Conclusions

The dramatic biological and chemical perturbations associated with the 1997–98 El Niño would not have been captured had it not been for in situ sensors on moorings, regular ship visits to service the moorings, and remote sensing of chlorophyll. Future equatorial Pacific observing strategies should include additional moorings in the TAO array equipped with biological and chemical sensors. Novel sensors for macronutrients and iron, presently under development, together with instruments that measure phytoplankton physiological status (50), would provide data to further elucidate the processes that drive the dramatic biogeochemical fluctuations in this region. Continued development of biogeochemical models will also be needed.

References and Notes

- R. A. Feely et al., *J. Geophys. Res.* **92**, 6545 (1987).
- F. P. Chavez, P. G. Strutton, M. J. McPhaden, *Geophys. Res. Lett.* **25**, 3543 (1998).
- C. R. McClain, M. L. Cleave, G. C. Feldman, W. W. Gregg, S. B. Hooker, *Sea Technol.* (September 1998).
- M. J. McPhaden, *Science* **283**, 950 (1999).
- J. R. Toggweiler and S. Carson, in *Upwelling the Ocean: Modern Processes and Ancient Records*, C. P. Summerhayes et al., Eds. (Wiley, Chichester, UK, 1995), pp. 337–360.
- R. A. Kerr, *Science* **280**, 522 (1998).
- R. A. Madden and P. R. Julian, *J. Atmos. Sci.* **28**, 702 (1971).
- K.-M. Lau and P. H. Chan, *Bull. Am. Meteorol. Soc.* **67**, 533 (1986).
- C. Jones, D. E. Waliser, C. Gautier, *J. Clim.* **11**, 1057 (1998).
- W. S. Kessler and M. J. McPhaden, *Deep Sea Res. Part II* **42**, 295 (1995).
- T. P. Barnett, M. Latif, E. Kirk, E. Roeckner, *J. Clim.* **4**, 487 (1991).
- R. A. Weller and S. P. Anderson, *J. Clim.* **9**, 1959 (1996).
- M. F. Cronin and M. J. McPhaden, *J. Geophys. Res.* **102**, 8533 (1997).
- K. E. Brainerd and M. C. Gregg, *J. Geophys. Res.* **102**, 10437 (1997).
- J. S. Godfrey et al., *J. Geophys. Res.* **103**, 14395 (1998).

- J. Picaut, M. Ioualalen, C. Menkes, T. Delcroix, M. J. McPhaden, *Science* **274**, 1486 (1996).
- M. J. McPhaden and J. Picaut, *Science* **250**, 1385 (1990).
- J. Picaut and T. Delcroix, *J. Geophys. Res.* **100**, 18393 (1995).
- W. M. Smethie Jr., T. Takahashi, D. W. Chipman, J. R. Ledwell, *J. Geophys. Res.* **90**, 7005 (1985).
- P. P. Tans, I. Y. Fung, T. Takahashi, *Science* **247**, 1431 (1990).
- T. Takahashi et al., *Proc. Natl. Acad. Sci. U.S.A.* **94**, 8292 (1997).
- F. P. Chavez, K. R. Buck, S. K. Service, J. Newton, R. T. Barber, *Deep Sea Res. Part II* **43**, 835 (1996).
- C. D. Keeling and R. Revelle, *Meteoritics* **20**, 437 (1985).
- H. Y. Inoue and Y. Sugimura, *Tellus* **44**, 1 (1992).
- C. Goyet and E. T. Peltzer, *Mar. Chem.* **45**, 257 (1994).
- N. Lefevre, C. Andrie, Y. Dandonneau, G. Reverdin, M. Rodier, *J. Geophys. Res.* **99**, 12639 (1994).
- A. M. E. Winguth et al., *Global Biogeochem. Cycles* **8**, 39 (1994).
- Y. Dandonneau, *Deep Sea Res. Part II* **42**, 349 (1995).
- D. Meyers and J. J. O'Brien, *Eos* **76**, 533 (1995).
- D. E. Archer et al., *Deep Sea Res. Part II* **43**, 779 (1996).
- R. Wanninkhof, R. A. Feely, H. Chen, C. Cosca, P. P. Murphy, *J. Geophys. Res.* **101**, 16333 (1996).
- K. Wyrki, *J. Phys. Oceanogr.* **11**, 1205 (1981).
- F. P. Chavez and R. T. Barber, *Deep Sea Res.* **34**, 1229 (1987).
- J. H. Martin et al., *Nature* **371**, 123 (1994).
- K. H. Coale et al., *Nature* **383**, 495 (1996).
- R. T. Barber and F. P. Chavez, *Science* **222**, 1203 (1983).
- R. T. Barber and F. P. Chavez, *Nature* **319**, 279 (1986).
- D. G. Foley et al., *Deep Sea Res. Part II* **44**, 1801 (1997).
- F. P. Chavez and S. L. Smith, in *Upwelling in the Ocean: Modern Processes and Ancient Records*, C. P. Summerhayes et al., Eds. (Wiley, Chichester, UK, 1995), pp. 149–169.
- P. G. Falkowski, R. T. Barber, V. Smetacek, *Science* **281**, 200 (1998).
- F. P. Chavez and J. R. Toggweiler, in *Upwelling in the Ocean: Modern Processes and Ancient Records*, C. P. Summerhayes et al., Eds. (Wiley, Chichester, UK, 1995), pp. 313–320.
- D. Halpern, R. A. Knox, D. S. Luther, *J. Phys. Oceanogr.* **18**, 1415 (1988).
- R. M. Gordon, K. H. Coale, K. S. Johnson, *Limnol. Oceanogr.* **42**, 419 (1997).
- K. S. Johnson, R. M. Gordon, K. H. Coale, *Mar. Chem.* **57**, 137 (1997).
- The range of iron to carbon ratios reported in Johnson et al. (44) from laboratory experiments was 2 to $100 \mu\text{mol}$ of Fe per mol of C.
- J. J. McCarthy, C. Garside, J. L. Nevins, R. T. Barber, *Deep Sea Res. Part II* **43**, 1065 (1996).
- W. P. Cochlan and R. M. Kudela, *Eos* **76**, 177 (1996).
- R. W. Eppley, F. P. Chavez, R. T. Barber, *J. Geophys. Res.* **97**, 655 (1992).
- F. Chai, S. T. Lindley, R. T. Barber, *Deep Sea Res. Part II* **43**, 1031 (1996).
- Z. S. Kolber, O. Prasil, P. G. Falkowski, *Biochim. Biophys. Acta Bioenergetics* **1367**, 88 (1998).
- J. A. Yoder, S. G. Ackleson, R. T. Barber, P. Flament, W. M. Balch, *Nature* **371**, 689 (1994).
- We wish to thank the officers and crew of the *Ka'imimoana* for support of the mooring and ship-based measurements; K. Angstadt, K. Baldwin, P. Bernhardt, J. Kahn, D. Sweeney, and K. Treese for assistance in collecting the in situ chlorophyll and nutrient data; and R. Herliem, M. Kelley, M. Pickerill, P. Walz, and the Monterey Bay Aquarium Research Institute (MBARI) machine shop for support of the MBARI mooring program. Financial support for this work was provided by the NOAA Office of Global Programs, the NASA SIMBIOS program, and the David and Lucile Packard Foundation.

14 June 1999; accepted 25 October 1999

LINKED CITATIONS

- Page 1 of 2 -



You have printed the following article:

Biological and Chemical Response of the Equatorial Pacific Ocean to the 1997-98 El Nino

F. P. Chavez; P. G. Strutton; G. E. Friederich; R. A. Feely; G. C. Feldman; D. G. Foley; M. J. McPhaden

Science, New Series, Vol. 286, No. 5447. (Dec. 10, 1999), pp. 2126-2131.

Stable URL:

<http://links.jstor.org/sici?sici=0036-8075%2819991210%293%3A286%3A5447%3C2126%3ABACROT%3E2.0.CO%3B2-Y>

This article references the following linked citations:

References and Notes

⁴ **Genesis and Evolution of the 1997-98 El Nino**

Michael J. McPhaden

Science, New Series, Vol. 283, No. 5404. (Feb. 12, 1999), pp. 950-954.

Stable URL:

<http://links.jstor.org/sici?sici=0036-8075%2819990212%293%3A283%3A5404%3C950%3AGAEOT1%3E2.0.CO%3B2-7>

⁶ **Models Win Big in Forecasting El Nino**

Richard A. Kerr

Science, New Series, Vol. 280, No. 5363. (Apr. 24, 1998), pp. 522-523.

Stable URL:

<http://links.jstor.org/sici?sici=0036-8075%2819980424%293%3A280%3A5363%3C522%3AMWBIFE%3E2.0.CO%3B2-%23>

¹⁶ **Mechanism of the Zonal Displacements of the Pacific Warm Pool: Implications for ENSO**

J. Picaut; M. Ioualalen; C. Menkes; T. Delcroix; M. J. McPhaden

Science, New Series, Vol. 274, No. 5292. (Nov. 29, 1996), pp. 1486-1489.

Stable URL:

<http://links.jstor.org/sici?sici=0036-8075%2819961129%293%3A274%3A5292%3C1486%3AMOTZDO%3E2.0.CO%3B2-Z>

¹⁷ **El Nino-Southern Oscillation Displacements of the Western Equatorial Pacific Warm Pool**

M. J. McPhaden; J. Picaut

Science, New Series, Vol. 250, No. 4986. (Dec. 7, 1990), pp. 1385-1388.

Stable URL:

<http://links.jstor.org/sici?sici=0036-8075%2819901207%293%3A250%3A4986%3C1385%3AENODOT%3E2.0.CO%3B2-B>

NOTE: *The reference numbering from the original has been maintained in this citation list.*

LINKED CITATIONS

- Page 2 of 2 -



²⁰ **Observational Constraints on the Global Atmospheric CO₂ Budget**

Pieter P. Tans; Inez Y. Fung; Taro Takahashi

Science, New Series, Vol. 247, No. 4949. (Mar. 23, 1990), pp. 1431-1438.

Stable URL:

<http://links.jstor.org/sici?sici=0036-8075%2819900323%293%3A247%3A4949%3C1431%3AOCOTGA%3E2.0.CO%3B2-N>

²¹ **Global Air-Sea Flux of CO₂ : An Estimate Based on Measurements of Sea-Air pCO₂ Difference**

Taro Takahashi; Richard A. Feely; Ray F. Weiss; Rik H. Wanninkhof; David W. Chipman; Stewart C. Sutherland; Timothy T. Takahashi

Proceedings of the National Academy of Sciences of the United States of America, Vol. 94, No. 16. (Aug. 5, 1997), pp. 8292-8299.

Stable URL:

<http://links.jstor.org/sici?sici=0027-8424%2819970805%2994%3A16%3C8292%3AGAFOCA%3E2.0.CO%3B2-X>

³⁶ **Biological Consequences of El Nino**

Richard T. Barber; Francisco P. Chavez

Science, New Series, Vol. 222, No. 4629. (Dec. 16, 1983), pp. 1203-1210.

Stable URL:

<http://links.jstor.org/sici?sici=0036-8075%2819831216%293%3A222%3A4629%3C1203%3ABCOEN%3E2.0.CO%3B2-J>

⁴⁰ **Biogeochemical Controls and Feedbacks on Ocean Primary Production**

Paul G. Falkowski; Richard T. Barber; Victor Smetacek

Science, New Series, Vol. 281, No. 5374. (Jul. 10, 1998), pp. 200-206.

Stable URL:

<http://links.jstor.org/sici?sici=0036-8075%2819980710%293%3A281%3A5374%3C200%3ABCAFOO%3E2.0.CO%3B2-C>